Microstructure and wear properties of YT758/ CuZnNi hardfacing materials[①]

WANG Xin-hong(王新洪)[1], ZHANG Min(张　敏)[2],

ZOU Zeng-da(邹增大)[1], QU Shi-yao(曲仕尧)[1]

(1. School of Materials Science and Engineering, Shandong University,

Ji'nan 250061, China;

2. School of Mechanical Engineering, Shandong University, Ji'nan 250061, China)

Abstract: Hardfacing materials containing YT758 hardmetal particles cemented by Cu-based alloy was deposited on the substrate to produce milling tools by oxy-acetylene flame process. Microstructure and wear properties of the hardfacing layers were analyzed by scanning electron microscopy (SEM) and electron dispersion X-ray spectroscopy(EDXS) and wear test. The results show that inter-diffusion zone is found at the interface of YT758/CuZnNi, which promises to improve the bonding strength of YT758/CuZnNi. The wear resistance of YT758/CuZnNi hardfacing layers is higher than that of YG8/CuZnNi hardfacing layers. The working efficiency of the milling tools strengthened by YT758/CuZnNi is approximately 2－3 times higher than that strengthened by YG8/CuZnNi.

Key words: wear properties; hardmetal; hardfacing materials; CuZnNi alloy; milling tools

CLC number: TG 455　　　　　　　　　**Document code:** A

---

1 INTRODUCTION

Milling tools are widely used to mill the fallen objects (such as tooth wheel, slipdog, oil tube and drill pipe) away in oil well. In general, the depth of the objects inside the oil well is about 2 000－5 000 m, the rotary speed of the milling tools is about 80－120 r/min and downhole load is about 5－30 kN. Additionally, high velocity slurry fluids are used to cool the tools and entrain the debris of the fallen objects during the milling[1-3]. As a result, the milling tools suffer from a severe wear and abrasion in service. In order to prolong the life of the tools, hardfacing materials with high wear resistance must be deposited on the surface of the milling tools.

In recent years, some hardfacing materials containing sintered WC-Co hardmetals cemented by Ag-based or Cu-based alloy have been applied in oil well for workover[4-8], such as WC-8Co/AgCuZn, WC-8Co/CnZnMn and WC-10Co/CuZnNi. Due to the low melting point of the matrix of the hardfacing materials, they can be deposited on the substrate by means of oxy-acetylene flame[9]. The WC-Co hardmetals have good bending strength and toughness; however, the hardness of WC-Co hardmetals is lower than that of WC-TiC-Co hardmetals when the content of Co is the same. On the other

hand, WC particles are easy to be oxidized and decomposed during the hardfacing and milling, giving rise to the formation of W_2C and $Co_x W_y C_z$ compounds[10, 11]. Such transformations affect the wear resistance of the depositing layers obviously. Therefore, a new type of hardfacing material is necessary to improve the quality of the milling tools.

In this paper, a new type of hardfacing material for the milling tools was developed, which contained of WC-8TiC-3TaC-8Co(YT758) hardmetals and CuZnNi alloy, and the microstructure and wear properties of the hardfacing material were investigated.

2 EXPERIMENTAL

2.1 Composition of materials

The chemical composition and mechanical performance of YT758 and YG8 are shown in Table 1.

The YG8 hardmetal belongs to the WC-Co series in which WC is only the hard phase and Co is the cohesive phase, however, the YT758 hardmetal belongs to the WC-TiC-Co series in which WC, TiC and (W, Ti)C solid solutions etc are the hard phases and Co is the cohesive phase. Cu-Zn-Ni alloy with a melting point of 890－920 ℃ was used as the matrix of the composite hardfacing materi-

Table 1   Composition and mechanical performance of hardmetal

Hardmetal	Composition(mass fraction)/ %					Hardness(HRA)	Density/(g · cm^{-3})	Bending strength/ MPa
	TiC	TaC(NbC)	Co	Cr$_3$C$_2$	WC			
YT758	8	3 ~ 4	8	0. 5	Bal.	92	13. 2	1 960
YG8	–	–	8	–	92	89	14. 75	2 520

als. The composition of the alloy is 46% ~ 52% Cu, 8% ~ 12% N and Zn balance(mass fraction). A brazing flux QJ130 is used to improve the wetting ability of hardmetals and Cu-based alloy. The composition of the flux is 76% ~ 79% H$_3$NO$_3$, 16% ~ 18% Na$_3$B$_4$O$_7$ and AlPO$_3$ balance(mass fraction).

2. 2   Oxidation test

Oxidation tests of hardmetal in air were carried out in an electric furnace maintained at the desired temperature(±1 ℃). The sample was machined to blocks in size of 16 mm × 10 mm × 5 mm, weighed accurately and placed in a high-purity alumina boat, then directly introduced in the hot zone of the furnace at a predetermined operating temperature. After the prescribed period, the sample together with its boat was removed from the furnace, cooled to room temperature, then reweighed accurately. In order to measure the thickness of the oxide layer, the oxide was removed from the hardmetals after oxidation, and the samples were rinsed by ultrasonic cleaning with acetone. The average thickness was calculated from the formula $\Delta H = (H_1 - H_2)/2$, where ΔH is the thickness of the oxide layer, and H_1 and H_2 are the thickness of the hardmetals before and after oxidation, respectively.

2. 3   Hardfacing processing and microstructure test

The mixture of 60% (mass fraction) hardmetal particles and 40% (mass fraction) CuZnNi alloy was used as the raw materials for preparing composite welding rod. The size of hardmetal particles is about 3 ~ 5 mm. The composite welding rod was formed inside an electric furnace. The heating temperature was 920 ~ 940 ℃ and the holding time was 15 ~ 20 min, then a slow cooling process outside of the furnace was followed. More details of the experimental procedure was provided elsewhere[12, 13].

The composite welding rod was deposited onto the substrate of AISI 1045 steel by using oxy-acetylene flame. The neutral flame or slight carburizing flame was set in the experiment.

A series of specimens were cut from the hardfacing layers. The microstructure was observed by scanning electron microscopy(SEM), the chemical composition was analyzed by using electron disper-

sion X-ray spectroscopy(EDXS), and the structure of hardfacing layer was analyzed by X-ray diffractometry(XRD) at room temperature.

2. 4   Wear test

Slurry erosive wear tests were carried out on a MSL-23 type water slag wear tester. The samples were machined to blocks with sizes of 57 mm × 26 mm × 6 mm. The testing abrasive was quartz, and the particle sizes of the quartz were 50 ~ 70 μm. The testing parameters were: load 98 N, wheel rotation velocity 192 r/ min, wheel diameter 178 mm. The mass ratio of abrasive and water was 3 : 2 in the slurry. Tests were carried out up to 30 min with mass loss measured at regular time intervals of 5 min. In all the wear tests, the mass of the samples was measured after washing and cleaning the samples by water and acetone.

The abrasive wear tests were performed on a MM-200 block-on-ring tester under dry sliding conditions. The sliding ring(hardmetal, hardness 91 HRA) with 40 mm in diameter was used as counter-body. It was polished to produce a final surface roughness of 0. 01 μm. The samples were machined to blocks with sizes of 20 mm × 10 mm × 10 mm and with surface roughness of 0. 08 μm. Wear tests were performed under a sliding speed of 8. 4 mm/ s, a normal load of 100 ~ 500 N and sliding distance 750 m. The wear resistance was determined by measuring the mass loss after a certain time interval on an analytical balance with a precision of ±0. 01 mg. Subsequently, the mass loss of the block specimens was converted to the wear volume.

3   RESULTS AND DISCUSSION

3. 1   Oxidation resistance of hardmetal

Fig. 1(a) shows the mass gains of hardmetals at different temperatures for 2 h. The relation of oxidation layer thickness versus time for the hardmetal samples oxidized in air at 800 ℃ is shown in Fig. 1(b). As is shown, the mass change of hardmetals exposed to air is strongly dependent on the oxidation temperature, time and type of hardmetal. The oxidation of the hardmetal is not serious when the exposed temperature is below 700 ℃. However, when the exposed temperature is higher

than 700 ℃, the oxidation rate increases remarkably. With the increase of exposed temperature and time, the mass gain of hardmetal increases accordingly. It is also found that the mass gain of YT758 hardmetal is less than that of YG8. This indicates that YT758 hardmetal possesses a higher oxidation resistance than YG8.
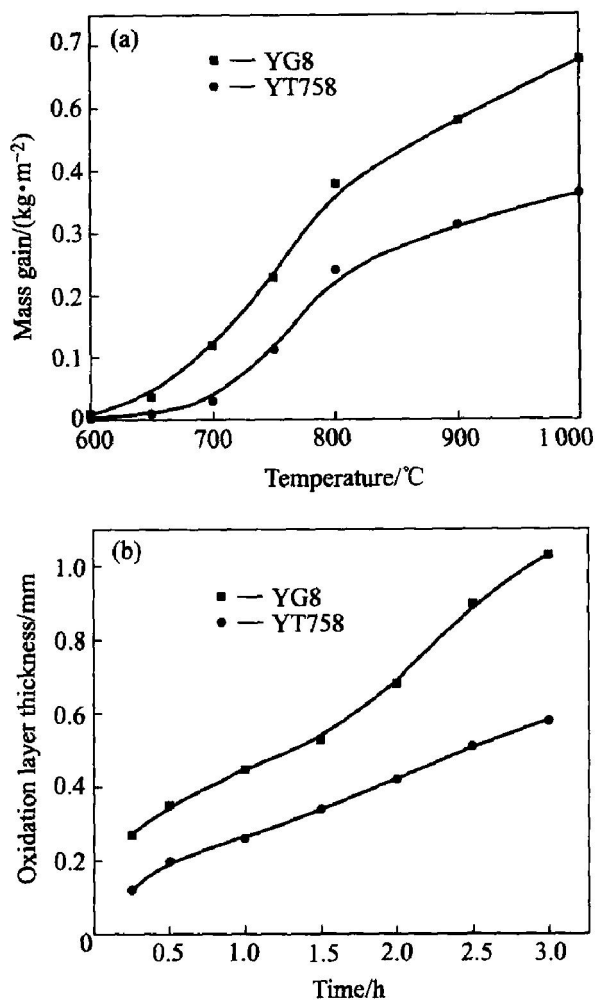

Fig. 1 Oxidation behavior of hardmetal
(a) —Mass gain of hardmetal as function of temperature for 2 h;
(b) —Oxidation layer thickness as function of time at 800 ℃

XRD-data of YG8 oxidized surface show that the oxidation is composed of WO_3 and $CoWO_4$. However, the XRD-data of YT758 oxidized surface show the presence of TiO_2, WO_3 and $CoWO_4$. Those oxidation phases will result in the destruc-

tion of carbide cohesive phase and decrease the hardness of hardmetal. Therefore, it is important to protect the hardmetal during heating process. In addition, for YT758 hardmetal, a dense oxidation thin film is found on the surface of hardmetal. It coveres on the surface of hardmetal and avoides the hardmetal to be oxidized further. Table 2 shows the hardness variations of hardmetal before and after heating under different protective conditions. This indicates that reinforcing protection of hardmetal can decrease the oxidation of the hardmetal and improve the properties of hardmetal.

3. 2 Milling tools and microstructure of hardfacing layer

Fig. 2 shows a typical Junk-milling tool. It is designed for milling stationary obstructions. The tool is deposited with YT758 hardmetal cemented by Cu-based alloy composite hardfacing materials. It can be used to mill tubing, cemented drill collars, drill pipes, etc. The tool is accomplished by sliding, tearing and gouging motions of the cutter elements on the fallen objects, which leads the milling tools to suffer from severe wear and erosion.
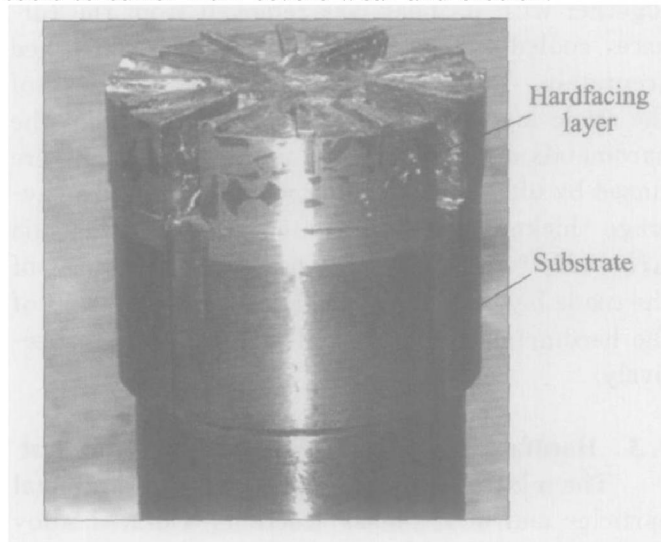

Fig. 2 Macromorphology of Junk-milling tool

According to the observation of SEM, the matrix of the hardfacing layer is mainly composed of fine α and β phases. The hardmetal is surrounded by α and β phases. The size of hardmetal is almost unchanged from that in its original state. The

Table 2 Hardness variation of hardmetals before and after heating

Type	Exposed temperature/ ℃	Exposed time/ h	Hardness before heating(HRA)	Hardness after heating(HRA)		
				Without protection	Flux protection	Protection in Ar
YT758	1 000	2	92, 92.5, 92	68, 66, 65, 67.5	91, 91.5, 91, 91.5	90, 90.5, 91.5, 91
YG8	1 000	2	89, 88.5, 89	45, 50, 45, 40.5	88, 88.5, 87, 88.5	87, 89, 88.5, 88

phase constitution of the hardfacing layers determined by X-ray diffraction consists of WC, TiC, TaC, α, β, CuNi and Co.

Typical interfacial microstructure morphologies of YT758/CuZnNi and YG8/CuZnNi are shown in Figs. 3(a) and (b), respectively. It can be seen that there is a clear interface zone between the YT758 hardmetal and matrix alloy(Fig. 3(a)). The interface of the YT758 hardmetals matches well with the Cu-based alloy. There are no obvious defects near the interface, such as porosities, microcracks or inclusions. However, there exists some loose structure at the interface of YG8 hardmetal and Cu-based. It will do harm to the impact properties and wear resistance of the hardmetal.
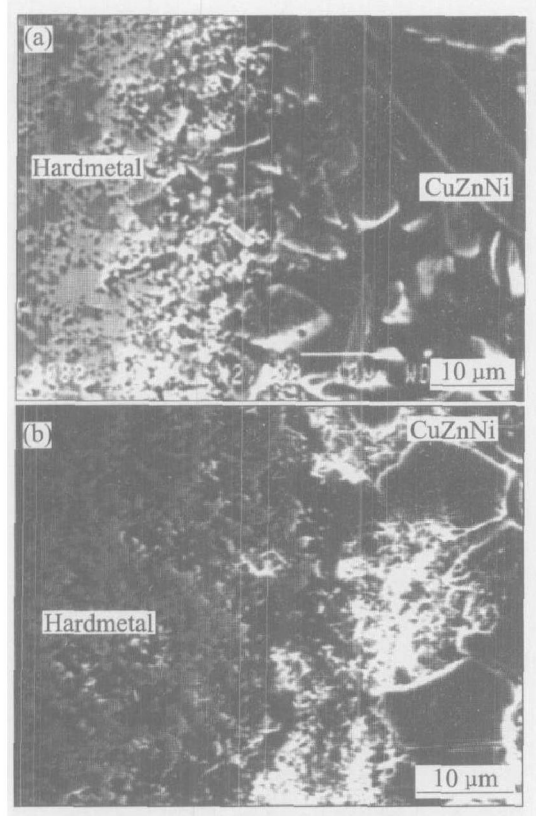

Fig. 3   Interfacial microstructures
(a) —YT758/CuZnNi; (b) —YG8/CuZnNi

Fig. 4   SEM morphology and elemental distributions of interface of YT758/CuZnNi
(a) —Line distribution of W and Ni;
(b) —Line distribution of Ti, Cu, Zn;
(c) —Face distribution of Co

The elemental distributions at the interface of YT758/CuZnNi are shown in Fig. 4. It shows that the distribution curves are rising or falling gradually at the interface. Nickel (Ni) diffuses into the hardmetal surface layer, tungsten (W) and cobalt (Co) diffuse into the matrix metal. There exits an inter-diffusion zone at the interface. This is proprtious for improving the bonding strength of the hardmetal and Cu-based alloy.

The variation of slurry wear mass loss with sliding time for hardfacing layers at slurry concentration of 60% sand in water is shown in Fig. 5. It can be seen that the wear mass loss increases with the increasing sliding time. However, the layer
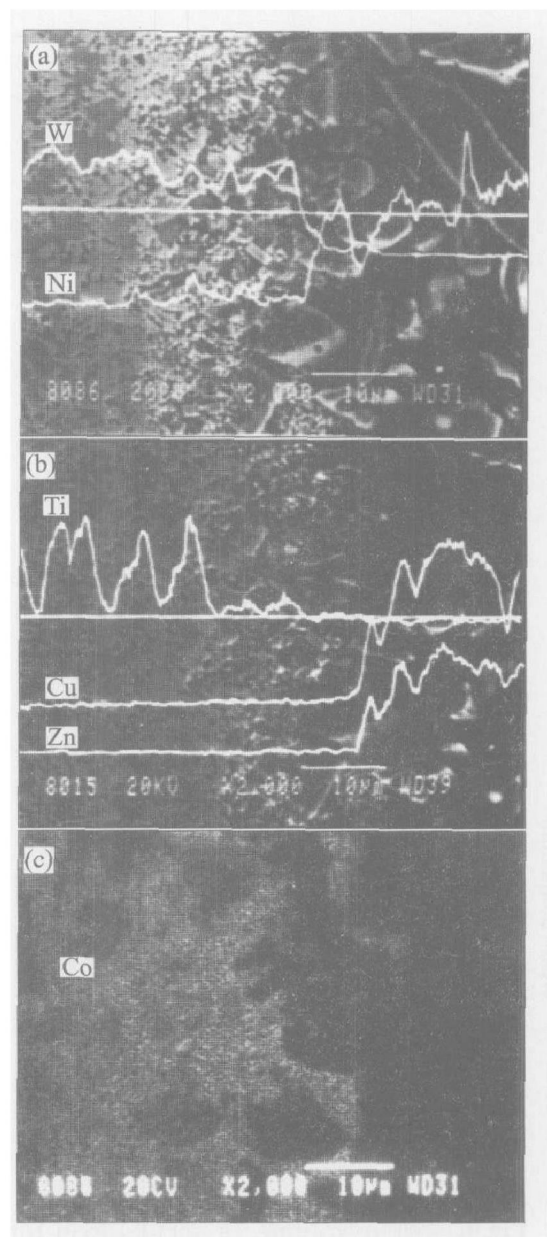
strengthened by YT758/CuZnNi shows greater wear resistance than that by YG8/CuZnNi. This may be attributed to higher hardness and less decomposition of YT758 hardmetal primarily.

The friction wear behavior of the hardfacing layers is given in Fig. 6. It illustrates the effect of the applied load on the wear resistance of the hardfacing layers at room temperature. It can be seen that the increase in load from 100 N to 500 N produces a 200% increase in total wear volume. At lower loads, comparatively low wear volume exists, indicating the regime of mild wear. At higher loads, the materials exhibit a rapid increase in wear volume, indicating the operation of a more sever regime of wear. The increase of wear volume with rise of the load can be explained in the following
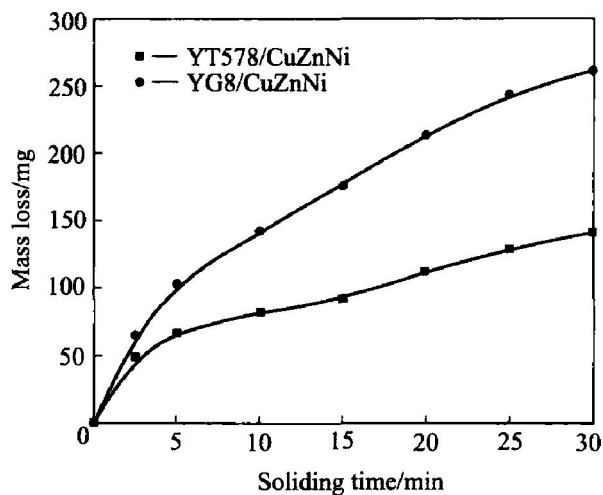
Fig. 5 Mass loss vs sliding time of
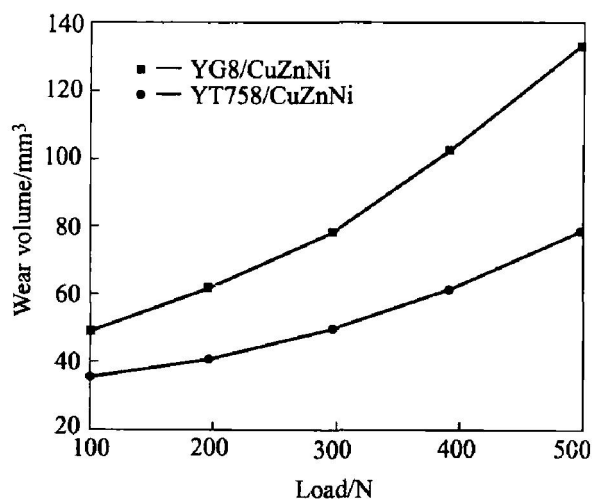hardmetal cemented by Cu-based alloy
hardfacing layers in slurry

Fig. 6 Wear volume vs normal load for
YT758/ CuZnNi and YG8/ CuZnNi
hardfacing layers

way: firstly, at higher loads, the adhesive effect of cold welding will increase, which causes a higher degree of material removal from the hardfacing layer; secondly, the contact stress will also go up with the load, which results in favor cracking and hence higher levels of plastic deformation of matrix and fracture of hardmetal in the hardfacing layer; finally, at higher loads, the frictional heating will be higher, which will promote the oxidative processes.

Fig. 6 also shows that the wear volume of the YT758/ CuZnNi hardfacing layers is a factor of 1. 5 ⁻ 2 times lower than that of YG8/ CuZnNi and gives a much lower increase with increasing of the normal load. This indicates that YT758/ CuZnNi hardfacing layers provide a better wear resistance than that of YG8/ CuZnNi. This may be ascribed to that YT769 has higher hardness than YG8 hardmetal. On the other hand, there exists good inter-

facial microstructure between YT758 hardmetal and CuZnNi matrix, which improves the bond strength between hardmetal and matrix, thus the fallen of the hardmetal can be avoided effectively during wear.

The SEM micrographs of the worn scar of the region around the interface of YT758 and CuZnNi under various normal loads are shown in Figs. 7(a) ⁻(c). It can be observed that plastic deformation and groove form in the matrix, and hardmetal serves as hard barriers and interrupts the scratching. A few microcracks of hardmetal in various directions are observed at the interface. This indicates a brittle fracture of single grain carbide particles of hardmetal during sliding. When the cracks propagate, carbide particles in the hardmetal are loosened and then pulled out. With increase of the load, the depth and width of grooves and the amounts of pullout carbide particles and wear debris increase.
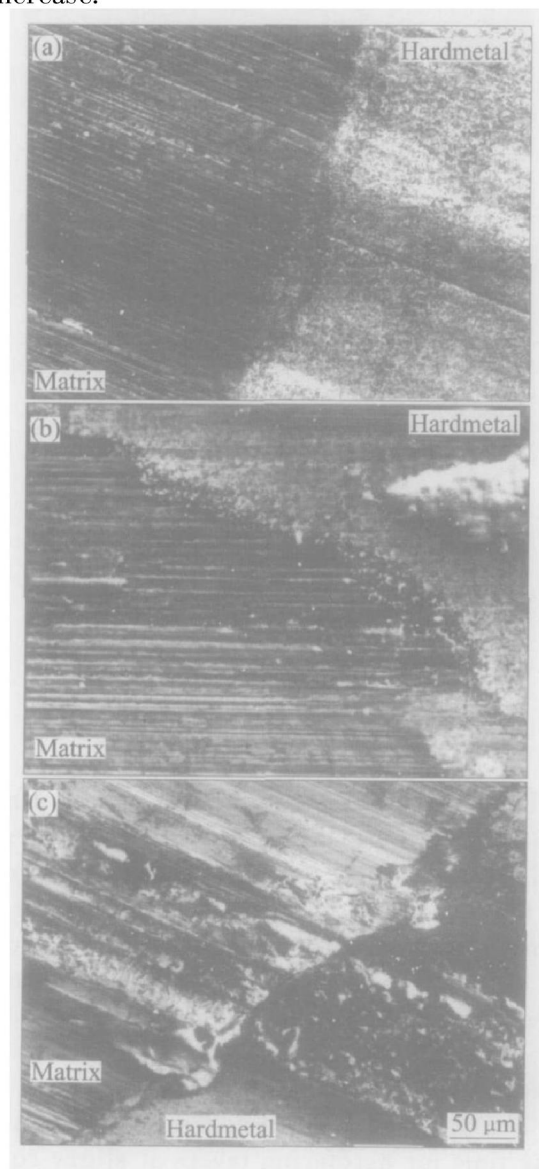

Fig. 7 Wear scars of composite surface coating
under different loads
(a) ⁻100 N; (b) ⁻200 N; (c) ⁻500 N

Fig. 8 shows the relationship between the milled length of the fallen objects and the milling time at downhole load of 9.8 kN and rotating speed of 80 r/min for a Junk-milling tool at the TK419 oil well. The working surface of the tools was deposited with a 15 mm thickness hardfacing material, and the outside diameter was 104 mm. The material of the fallen object was API 5CT J55 oil tube with a 73 mm diameter and a 6.3 mm (0.25-in) thickness. The chemical composition of the J55 oil tube was (mass fraction): 12% C, 45% Si, 150% Mn, 2.5% P, 2.0% S, 0.5% Nb, 0.5% V, 0.5% Ti, and its strength was 520 MPa[14]. The depth of the fallen objects inside the oil well was about 5 000 m. This indicates that YT758/ CuZnNi hardfacing material possesses a higher life than YG8/ CuZnNi. The working efficiency of the tools deposited YT758/ CuZnNi surface coating is 2 − 3 times higher than the ones deposited YG8/ CuZnNi.
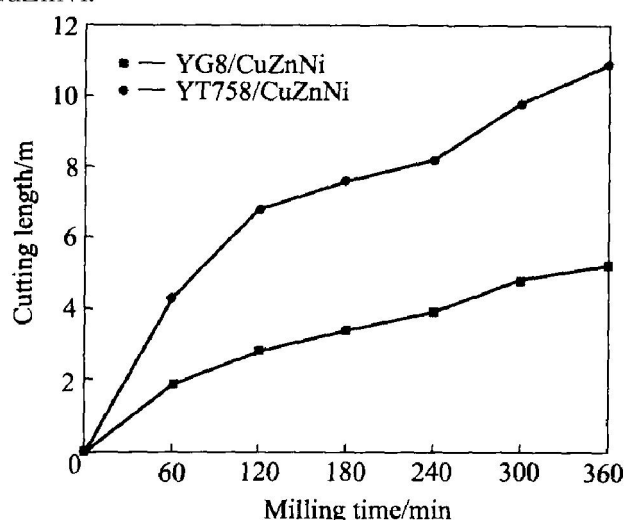

Fig. 8   Milling length of object versus time

Fig. 9 shows the macrograph of the worn surface of the tools deposited YT758 /CuZnNi and YG8/CuZnNi at rotating speed of 80 r/min and downhole force of 9.8 kN, respectively. Severe damage occurs on the hardfacing layer and the edge of the hardmetals lose their original geometry. There exist a lot of fall-off dimples in the YG8/ CuZnNi hardfacing layer. YG8 hardmetal is mainly composed of WC, which is easy to decompose and oxidize during the depositing process[15]. As a result, it not only reduces the microhardness of hardmetal but also changes the composition and microstructure of the YG8 hardmetal. The brittle phase of W_2C or Co_2W_4C is formed on the interface of YG8 and CuZnNi matrix, which decreases the impact toughness of hardmetal. Therefore some dimples of fall-off hardmetals are found in the surface of Junk-milling tool.
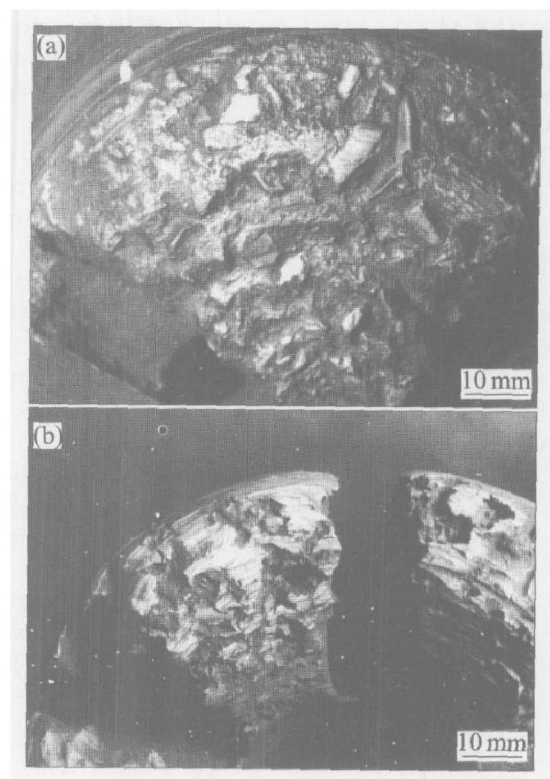

Fig. 9   Wear scars of milling shoe after used
(a) —YT758/ CuZnNi; (b) —YG8/ CuZnNi

4   CONCLUSIONS

1) In the YT758/ CuZnNi hardfacing layer, the hardmetals are surrounded by $\alpha + \beta$ phase. There exits an inter-diffusion zone at the interface of the hardmetal and CuZnNi matrix.

2) The wear resistance of the hardfacing layers decreases with the increase of normal load. The YT758/ CuZnNi hardfacing layer has a higher wear resistance than YG8/ CuZnNi hardfacing layer.

3) The Junk-milling tool deposited YT758/ CuZnNi hardfacing layer is found to possess a higher life and working efficiency than YG8/ CuZnNi. Severe damage occurs on the hardfacing layer and the edge of hardmetals loses their original geometry. There exist a lot of fall-off dimples in the YG8/ CuZnNi hardfacing layer.

REFERENCES

[1]   Baste U, Hartzell T, Engqvist H, et al. Surface damage on cemented carbide rock-drill buttons [J]. Wear, 2001, 249: 324 − 329.

[2]   Bailey S G, Perrott C M. Wear processed exhibited by WC-Co rotary cutters in milling [J]. Wear, 1974, 29 (1): 117 − 121.

[3]   Kembaiyan K T, Keshavan K. Combating fluid erosion and corrosion of drill bits using thermal spray coatings [J]. Wear, 1995, 186: 487 − 492.

[4]   Springer J. Pipe milling Tool Blade and Method of Dressing Same [P]. US 5012863, 1991.

[5]   Keshavan M K, Underwood L. Hardfacing materials

for milled tooth rock bits [J]. American Society of Mechanical Engineers, 1990, 27: 27－35.

[6] ZOU X M. The failure analysis of tooth-face strengthening materials of tri-cone drill and the study of new materials for tooth-face strengthening [J]. Cemented Carbide, 1995(8): 183－186. (in Chinese)

[7] LIU C J, TANG X W, CHEN H. Microstructure analysis of surface welding layer of cemented carbide on three cone bit [J]. Journal of Southwest Petroleum Institute, 2001, 23(2): 56－59 . (in Chinese)

[8] ZOU X M. Review of the WC strengthening materials for downhole tools [J]. Rare Metal and Cemented Carbide, 1995(9): 11－18. (in Chinese)

[9] SHI G Q, HUANG W Z. The study and application of hard alloy surfacing electrode [J]. Welding, 1984 (12): 14－17. (in Chinese)

[10] Karimi A, Verdon C. Hydroabrasive wear behaviour of high velocity oxyfuel thermally sprayed WC-M coatings [J]. Surface and Coatings Technology, 1993, 62(1－3): 493－498.

[11] HAN B Q, LI N. Synthesis of Al_2O_3/WC powder by aluminothermic reduction and carbonization method [J]. Trans Nonferrous Met Soc China, 2004, 14(2):

246－250.

[12] WANG X H, ZOU Z D, LI Y J, Development of a wear-resisting composite surfacing welding rod containing hardmetal [J]. Welding Technology, 1999, 28(3): 25－27. (in Chinese)

[13] WANG X H, ZOU Z D. Advances in the strengthened materials and welding technology for milling tools [J]. Materials for Mechanical Engineering, 2001, 25(4): 4－7. (in Chinese)

[14] American Petroleum Institute. 5CT Specification for Casing and Tubing(5th Edition) [M]. Washington: American Petroleum Institute, 1995. 6.

[15] ZHANG W K, ZHOU B X, CHEN D H, et al. Preparation and electrocatalytic properties of tungsten carbide electrocatalysts [J]. Trans Nonferrous Met Soc China, 2002, 12(6): 1015－1019.

[16] QU S Y, WANG X H, ZOU Z D. The heat damage mechanism of WC cemented carbide for hardfacing [J]. Trans of the China Welding Institution, 2001, 22(2): 85－88. (in Chinese)

(Edited by LI Xiang-qun)